Ferromagnetic Exchange Anisotropy from Antiferromagnetic Superexchange in the Mixed 3d-5d Transition-Metal Compound $Sr_{3}CuIrO_{6}$

Wei-Guo Yin, X. Liu, A. M. Tsvelik, M. P. M. Dean, M. H. Upton, Jungho Kim, D. Casa, A. Said, T. Gog, T. F. Qi, G. Cao, and J. P. Hill

Ferromagnetic Exchange Anisotropy from Antiferromagnetic Superexchange in the Mixed $3d - 5d$ Transition-Metal Compound $\text{Sr}_3\text{CuIrO}_6$

Wei-Guo Yin,[1, *] X. Liu,[2, 1] A. M. Tsvelik,[1] M. P. M. Dean,[1] M. H. Upton,[3]
Jungho Kim,[3] D. Casa,[3] A. Said,[3] T. Gog,[3] T. F. Qi,[4, 5] G. Cao,[4, 5] and J. P. Hill[1]

[1]*Condensed Matter Physics and Materials Science Department,*
Brookhaven National Laboratory, Upton, New York 11973, USA
[2]*Beijing National Laboratory for Condensed Matter Physics,*
and Institute of Physics, Chinese Academy of Sciences, Beijing 100190, China
[3]*Advanced Photon Source, Argonne National Laboratory, Argonne, Illinois 60439, USA*
[4]*Center for Advanced Materials, University of Kentucky, Lexington, Kentucky 40506, USA*
[5]*Department of Physics and Astronomy, University of Kentucky, Lexington, Kentucky 40506, USA*

We report a combined experimental and theoretical study of the unusual ferromagnetism in the one-dimensional copper-iridium oxide $\text{Sr}_3\text{CuIrO}_6$. Utilizing Ir L_3 edge resonant inelastic x-ray scattering, we reveal a large gap magnetic excitation spectrum. We find that it is caused by an unusual exchange anisotropy generating mechanism, namely strong ferromagnetic anisotropy arising from antiferromagnetic superexchange, driven by the alternating strong and weak spin-orbit coupling on the $5d$ Ir and $3d$ Cu magnetic ions, respectively. From symmetry consideration, this novel mechanism is generally present in systems with edge-sharing Cu^{2+}O_4 plaquettes and Ir^{4+}O_6 octahedra. Our results point to unusual magnetic behavior to be expected in mixed $3d - 5d$ transition-metal compounds via exchange pathways that are absent in pure $3d$ or $5d$ compounds.

The interest in strongly correlated electronic systems has recently been extended from $3d$ transition-metal compounds (TMCs) to $5d$ compounds. Usually the strength of electron correlation is characterized by the ratio of the local Coulomb repulsion to the electronic bandwidth. A large value of this ratio (~ 8) is common in $3d$ TMCs such as superconducting cuprates [1]. Since $5d$ orbitals are more extended in space and host weaker Coulomb interactions than $3d$ orbitals, $5d$ TMCs are generally expected to be weakly correlated. However, it has been pointed out [2–4] that the relative weakness of the Coulomb interaction is offset by the strong spin-orbit coupling (SOC), which is typically ~ 0.5 eV for $5d$ elements. This strong SOC leads to a significant splitting and narrowing of the electronic bands, and pushes $5d$ TMCs toward the strongly correlated regime. Indeed, the SOC-driven Mott metal-insulator transition was shown to exist in a variety of $5d$ iridium oxides [2–14]. An important consequence is the entanglement of the orbital and spin degrees of freedom in the resulting localized magnetic moments (termed 'isospins'), which can lead to unusual superexchange pathways and to new physics, for example, the proposed spin-liquid state as encoded in the Kitaev model [15] in the honeycomb-lattice $(\text{Li},\text{Na})_2\text{IrO}_3$ [7] and possible superconductivity in the square-lattice Sr_2IrO_4, which shows a similar magnetic ordering and dynamics to the cuprates [5].

The purpose of this letter is to demonstrate that materials containing *both* $3d$ and $5d$ magnetic ions can host new physics absent in either pure $3d$ or pure $5d$ compounds - because of the unique combination of unusual exchange pathways and special geometries, a result of the strong SOC of the $5d$ electrons and the differing coordinations of the $3d$ and $5d$ sites. Such materials will offer new avenues to engineer exotic magnetic behavior. To demonstrate this, we have chosen to study the one-dimensional copper-iridium oxide, $\text{Sr}_3\text{CuIrO}_6$, as a prototype for such mixed $3d - 5d$ systems. The crystal structure of this compound [Fig. 1(a)] is reminiscent of both the superconducting cuprates and iridium-based Mott insulators. Specifically, it contains with chains of alternating Cu and Ir the Cu^{2+} in a planar oxygen coordination and the Ir^{4+} in an octahedral oxygen coordination. The physical novelty of this material is demonstrated by the emergence of ferromagnetic order, which is rare in pure cuprates or iridates (the closely related materials $\text{Sr}_3\text{CuPtO}_6$ and $\text{Sr}_3\text{ZnIrO}_6$ are antiferromagnetic) and was used to synthesize random quantum spin chain paramagnetism in $\text{Sr}_3\text{CuIr}_{1-x}\text{Pt}_x\text{O}_6$ [16, 17]. There is to date no microscopic understanding of this unique phenomenon of ferromagnetism.

Here we use Ir L_3 edge resonant inelastic x-ray scattering (RIXS) [5, 14, 18, 28] to reveal a large gap magnetic excitation spectrum in $\text{Sr}_3\text{CuIrO}_6$, and show that it is well described by the effective $S = 1/2$ ferromagnetic Heisenberg model with an Ising-like exchange anisotropy. We present a microscopic derivation of this model, and find that the arrangement of alternating isospins and real spins on the edge-sharing $\text{Ir}^{4+}\text{O}_6\text{-Cu}^{2+}\text{O}_4$ chain leads to an unexpected effect, namely that the ferromagnetic anisotropy arises from the antiferromagnetic superexchange. Our results point to an entirely new class of
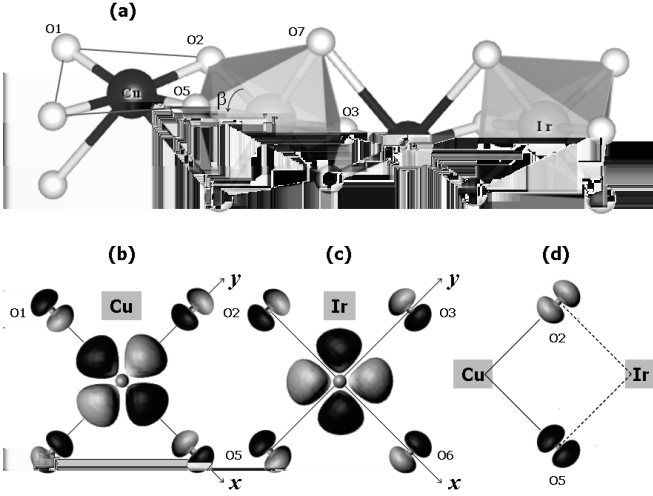
FIG. 1. (a) Cu-Ir chain of Sr_3CuIrO_6 where Cu^{2+} and Ir^{4+} are coordinated by an oxygen plaquette and octahedron, respectively. The IrO_6 octahedral tilting is denoted by $\alpha \simeq 150°$ and the octahedral distortion by $\beta \simeq 82°$. In the ideal case of $\alpha = 180°$ and $\beta = 90°$, the O2 and O5 and their neighboring Cu and Ir atoms form a square. (b) and (c) Schematic drawings of Cu $3d_{x^2-y^2}$ and Ir $5d_{xy}$ Wannier orbitals, ϕ_{Cu} and $\phi_{Ir,xy}$, respectively. Note the considerable tails on the oxygen sites due to the metal-oxygen hybridization. (d) Schematic map of the overlap density, $\rho = \phi_{Cu}\phi_{Ir,xy}$. Red (blue) represents positive (negative) values.
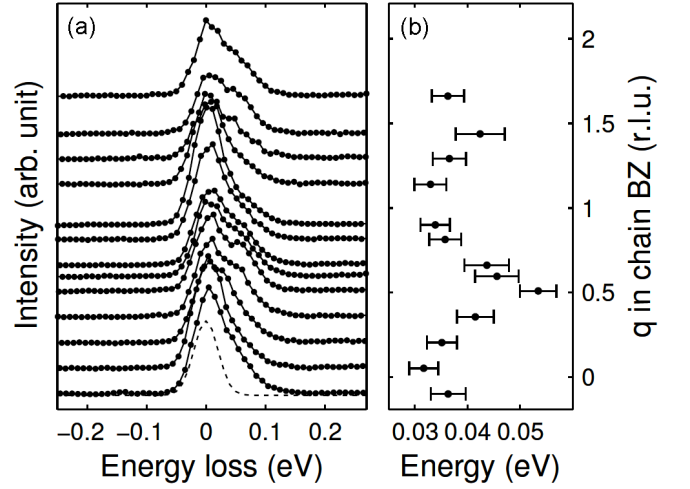

FIG. 2. (a) RIXS spectra for different momentum transfer along the chain direction, compared with the off-resonant elastic line (dotted line). (b) the extracted magnetic dispersion from the scans shown in (a). The scans in (a) are offset to match with their wavevector transfer along the chain direction presented in (b).

magnetic behavior in mixed $3d - 5d$ TMCs.

RIXS measurements.—The energy and momentum dependence of the magnetic excitation spectrum in a self-flux-grown Sr_3CuIrO_6 single crystal was studied by using Ir L_3 edge RIXS, for which dipole transitions excite and deexcite a $2p_{3/2}$ core-electron to the $5d$ orbitals [5, 14, 18]. The measurements were carried out at beamline 9-ID, Advanced Photon Source, in a horizontal scattering geometry. A Si(844) secondary monochromator and a R=2m Si(844) diced analyzer were utilized. The overall energy resolution of this setup was $\sim$ 45 meV (FWHM) and the momentum resolution was better than 0.07 of the Brillouin zone (BZ) length along the Cu-Ir chain direction. All data were collected at 7 K.

Fig. 2(a) shows the low-energy RIXS spectra for the momentum transfer q along the chain direction in the BZ in which the unit cell contains one Cu ion and one Ir ion. A shoulder appears near the elastic line and disperses along the chain direction. No dispersion is seen in this feature for momentum transfers perpendicular to the chain direction (not shown). We attribute this shoulder to a one-dimensional magnon mode. Its dispersion is plotted in Fig. 2(b), and shows two salient features: (i) The minimum energy located at the Γ point is not zero, but rather shows a large gap of $\sim$ 30 meV, comparable to the magnon bandwidth. (ii) The dispersive behavior follows the periodicity of the (one Ir plus one Cu) chain

unit cell very well, approximately in the form of $\cos(qa)$ where a is the nearest Ir-Ir distance.

These observations cannot be explained by conventional models. The simple linear chain ferromagnetic Heisenberg model proposed for this system [16] is gapless. In the related iridate Sr_3ZnIrO_6, two mechanisms have been proposed for a possible gap there. However, neither can be at work here. In the first, singlet dimers were proposed based on the alternating chain antiferromagnetic Heisenberg model [17]. However, this cannot occur in Sr_3CuIrO_6, since it is ferromagnetic. In the second, an Ising-like exchange anisotropy is added to the $S = 1/2$ Heisenberg model [19]. However, the magnon dispersion of the ferromagnetic model of this type, in which one does not distinguish between Cu and Ir atoms (i.e., the unit cell contains one magnetic ion), is in the form of $\cos(qa/2)$ [20, 21], in disagreement with the dispersion observed above. Our data thus require unconventional magnetism in this system, and make a general call for a new understanding of systems with mixed $3d - 5d$ magnetic ions.

Microscopic mechanism.—To understand the microscopic origin of the ferromagnetism and the anisotropy in this system, we start by analyzing the geometry and symmetry of the Cu-Ir chain.

A portion of a Cu-Ir chain of Sr_3CuIrO_6 is shown in Fig. 1(a). The Cu^{2+} ion is located at the center of an oxygen plaquette. The only magnetic orbital ϕ_{Cu} centered on a Cu^{2+} ion is of $x^2 - y^2$ symmetry and is antisymmetric with regard to the Cu-Ir mirror plane [Fig. 1(b)].

The Ir^{4+} ion lies in the center of an oxygen octahedron which shares an edge with neighboring CuO_4 plaquettes

and experiences tilting and an orthorhombic distortion characterized by angles $\alpha \simeq 150°$ and $\beta \simeq 82°$, respectively, as defined in Fig. 1(a). The octahedral ligand field renders the three Ir t_{2g} ($5d_{xy}$, $5d_{xz}$, and $5d_{yz}$) orbitals relevant to the low-energy physics, while the two unoccupied Ir e_g energy levels are ~ 3 eV higher [14]. We shall show below that the octahedral tilting and distortion are also relevant to the magnetism in Sr_3CuIrO_6, and that the role of the Ir $5d_{xy}$ orbital is completely different from those of the Ir $5d_{xz}$ and $5d_{yz}$ orbitals.

The Ir $5d_{xy}$ orbital, $\phi_{Ir,xy}$, is symmetric with regard to the Cu-Ir mirror plane [Fig. 1(c)], and thus orthogonal to ϕ_{Cu}, even in the presence of the octahedral tilting and distortion. As a result, electron hopping between these two orbitals is prohibited and so is the superexchange process. Thus, the leading magnetic interaction between them is the direct exchange interaction, J_F, which is ferromagnetic [23, 24]. From the measured magnon bandwidth (Fig. 2), we conclude that J_F is of order of dozens of meV. This is surprising, since direct exchange in TMCs is usually very small. The unusually large J_F comes from the fact that the tails of $\phi_{Ir,xy}$ and ϕ_{Cu} actually overlap well around each of O2 and O5 in Fig. 1(d) [22], similar to the large direct exchange ferromagnetism proposed for a Cu^{2+}-$(VO)^{2+}$ heterobinuclear complex [25].

By contrast, the Ir $5d_{xz}$ ($5d_{yz}$) orbital has a tail of p_z symmetry around O2 (O5); its overlap with ϕ_{Cu} is vanishing everywhere, leading to a negligible direct exchange. Actually, the Ir $5d_{xz}/5d_{yz}$ orbitals are not orthogonal to ϕ_{Cu} when α is tilted away from $180°$, and electron hopping between them is allowed. Therefore, the leading magnetic interaction between them is the antiferromagnetic superexchange.

The above considerations lead to the following effective magnetic Hamiltonian for Sr_3CuIrO_6:

$$
\begin{aligned}
H = \quad & -J_F \sum_{\langle \mathbf{m},\mathbf{n} \rangle} \vec{S}_{\mathbf{m},x^2-y^2} \cdot \vec{S}_{\mathbf{n},xy} \\
& + J_{AF} \sum_{\langle \mathbf{m},\mathbf{n} \rangle} \vec{S}_{\mathbf{m},x^2-y^2} \cdot (\vec{S}_{\mathbf{n},yz} + \vec{S}_{\mathbf{n},zx}) \\
& + \lambda \sum_{\mathbf{n}} \vec{L}_{\mathbf{n}} \cdot \vec{S}_{\mathbf{n}} + \Delta \sum_{\mathbf{n}\sigma} d^{\dagger}_{\mathbf{n},xy,\sigma} d_{\mathbf{n},xy,\sigma}, \quad (1)
\end{aligned}
$$

where $\mathbf{m}$ denotes a Cu site, $\mathbf{n}$ an Ir site, and $\langle \mathbf{m},\mathbf{n} \rangle$ means nearest neighbors. There is one hole at each site, as implied by Cu^{2+} and Ir^{4+}. $\vec{S}_{\mathbf{n},\gamma} = \sum_{\mu\nu} d^{\dagger}_{\mathbf{n},\gamma,\mu} \vec{\sigma}_{\mu\nu} d_{\mathbf{n},\gamma,\nu}/2$ where $\vec{\sigma}_{\mu\nu}$ is the Pauli matrix and $d_{\mathbf{n},\gamma,\mu}$ is the annihilation operator of an electron with spin $\mu = \uparrow, \downarrow$ (or $\pm$) and orbital $\gamma = xy, xz, yz$ on the Ir site $\mathbf{n}$. λ is the SOC constant on the Ir sites and Δ is the strength of the orthorhombic distortion of the IrO$_6$ octahedra. $-J_F < 0$ is the ferromagnetic direct exchange coupling between the Ir $5d_{xy}$ and Cu $3d_{x^2-y^2}$ orbitals. $J_{AF} > 0$ is the antiferromagnetic superexchange coupling between the Ir $5d_{xz}/5d_{yz}$ and Cu $3d_{x^2-y^2}$ orbitals.

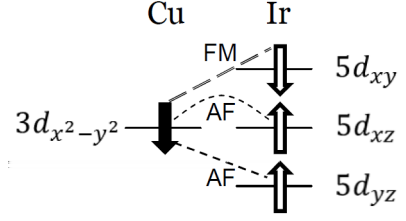The different types of magnetic interaction, J_{AF} and

FIG. 3. Schematic of unusual exchange pathways between a Cu down spin and an Ir down isospin. All the arrows indicate the real-spin orientations, and open arrows mean partial occupation in the isospin states [Eq. (2)]. Dashed lines indicate antiferromagnetic (AF) or ferromagnetic (FM) exchange; they cooperate to generate the ferromagnetic spin-isospin interaction. Ir $5d_{xz}$ and $5d_{yz}$ orbitals contribute only to the diagonal part of the exchange processes (see text), leading to the easy-z-axis anisotropy.

J_F, are usually expected to compete with each other. However, we show below from symmetry consideration that this understanding is qualitatively changed by the presence of strong λ. The three Ir t_{2g} orbitals form a reduced space with an effective orbital angular momentum $l_{\mathrm{eff}} = 1$ with its z component $l_z = 0$ for d_{xy} and $l_z = \pm 1$ for $id_{yz} \pm d_{zx}$ [26]. The leading energy scales $\lambda = 0.44$ eV and $\Delta = 0.31$ eV split them into three doublets with the lowest-energy one clearly separated from the other two by 0.58 and 0.81 eV, respectively [14]. The wave functions of the lowest-energy doublet are of the form [22]

$$
|\phi_{0,\eta}\rangle = \frac{1}{\sqrt{2+p^2}}(pd_{xy,\eta} + id_{yz,\bar{\eta}} + \eta d_{zx,\bar{\eta}}), \quad \eta = \pm, \quad (2)
$$

where $p = 0.65$ ($p = 0, 1$ for $\Delta = \infty, 0$, respectively). With the z component of total angular momentum $j_z = \pm 1/2$, they form an effective $S = 1/2$ 'isospin' on the Ir site, $\vec{s}_{\mathbf{n}} = \sum_{\eta\eta'} |\phi_{0,\eta}\rangle \vec{\sigma}_{\eta\eta'} \langle \phi_{0,\eta'}|/2$. Here we have adopted the same coordinate system for all the real spins and isospins in the lattice. Eq. (2) reveals that the Ir $5d_{xy}$ and $5d_{xz}/5d_{yz}$ orbitals have opposite real spin orientations ($s_z = \pm 1/2$) in the isospin basis, because $s_z = j_z - l_z$. Therefore, the tendency of the spin in the Ir $5d_{xy}$ ($5d_{xz}/5d_{yz}$) orbital to be parallel (antiparallel) to neighboring Cu spins can be satisfied simultaneously via this spin-orbit-coupled Kramers doublet, as illustrated in Fig. 3. Hence, the J_{AF} and J_F terms counterintuitively cooperate to generate the ferromagnetic interaction between Cu spins and Ir isospins.

Furthermore, we find that by symmetry the Ir $5d_{xy}$ and $5d_{xz}/5d_{yz}$ orbitals make completely different contributions to the isospin-flipping processes [from $\eta = +$ to $-$ or vice versa in Eq. (2)], in which $d_{xy,+} \leftrightarrow d_{xy,-}$ does not change l_z and $id_{yz,-} + d_{zx,-} \leftrightarrow id_{yz,+} - d_{zx,+}$ changes l_z by ± 2. Since $\vec{S}_{\mathbf{n},xy}$ and $\vec{S}_{\mathbf{n},yz} + \vec{S}_{\mathbf{n},zx}$ in Eq. (1) are l_z-preserving operators, the former contributes to the isospin-flipping processes and the latter does not. This means that the contributions of the J_F and J_{AF} terms

in Eq. (1) to the spin-isospin dynamics are isotropic and anisotropic, respectively. Thus, the strength of the resulting Ising-like exchange anisotropy is positively correlated with the relative importance of the Ir $5d_{xz}/5d_{yz}$ orbitals, which can be substantially enhanced by octahedral titling for increasing J_{AF}/J_F or by octahedral distortion ($\Delta > 0$) for increasing $1/p^2$, the relative weight of the Ir $5d_{xz}/5d_{yz}$ orbitals in $|\phi_{0,\eta}\rangle$.

It is noteworthy that in the context of the Kitaev model, an Ising-like ferromagnetic exchange between two Ir isospins due to the simultaneous presence of SOC and Hund's rule coupling was suggested for $(Li,Na)_2IrO_3$ [7]. We emphasize that the present symmetry-based mechanism for creating the Ising-like ferromagnetic exchange between a Cu spin and an Ir isospin is entirely different because it is independent of Hund's rule coupling.

To describe this strongly anisotropic spin dynamics, we derive from Eq. (1) the following effective $S = 1/2$ spin-isospin Hamiltonian [22]:

$$H_{eff} = H^{(0)} + H^{(2)},$$
$$H^{(0)} = -J_1 \sum_{\langle \mathbf{m},\mathbf{n} \rangle} \left\{ S_{\mathbf{m}}^x s_{\mathbf{n}}^x + S_{\mathbf{m}}^y s_{\mathbf{n}}^y + \gamma_1 S_{\mathbf{m}}^z s_{\mathbf{n}}^z \right\}, \quad (3)$$
$$H^{(2)} = -J_2 \sum_{\langle\langle \mathbf{m},\mathbf{m}' \rangle\rangle} \left\{ S_{\mathbf{m}}^x S_{\mathbf{m}'}^x + S_{\mathbf{m}}^y S_{\mathbf{m}'}^y + \gamma_2 S_{\mathbf{m}}^z S_{\mathbf{m}'}^z \right\},$$

where $\langle \mathbf{m},\mathbf{n} \rangle$ and $\langle\langle \mathbf{m},\mathbf{m}' \rangle\rangle$ mean the nearest Cu-Ir and Cu-Cu neighbors, respectively. $\vec{S}_{\mathbf{m}}$ is a shorthand notation of $\vec{S}_{\mathbf{m},x^2-y^2}$. $H^{(0)}$ and $H^{(2)}$ contain zeroth-order and second-order terms in perturbation theory, respectively. We find $J_2/J_1 \sim 0.1$; thus, $H^{(0)}$ governs main physics. $H^{(2)}$ is to be shown to have dramatic impact on the atom-specific magnon spectral weight. The strength of the derived exchange anisotropy, $\gamma_1 - 1 = (2/p^2)J_{AF}/J_F$, is proportional to J_{AF}/J_F and $1/p^2$, indeed.

Note that due to the difference of the (Landé) g-factors for spins and isospins an applied uniform magnetic field along the z axis is seen by the system as a staggered one. Indeed, the isospin's magnetic moment is $\mu_B(2\mathbf{S} - \mathbf{l})$ [26] and from Eq. (2) it follows that its g factor is $g_J = 2(p^2 - 4)/(p^2 + 2) = -2.96$ for the z component, in contrast to $g_S = 2$ of the Cu spin. As a result, the saturation magnetization is $\mu_B|g_J + g_S|/2 \simeq 0.5\mu_B$ per unit cell, close to the experimental value of $0.6\mu_B$ rather than $2\mu_B$ expected for a conventional system containing two unpaired electrons [17]. Thus our theory provides an explanation of this outstanding puzzle.

$H^{(0)}$ is integrable [20, 21]. Its spectrum consists of a fundamental magnon mode and multi-magnon bound states. The single magnon dispersion is $\omega(q) = J_1[\gamma_1 - \cos(qa/2)]$, where a is the nearest Ir-Ir distance and q a momentum along the Cu-Ir chain. This expression coincides with the spin-wave dispersion calculated using the Holstein-Primakoff transformation. Together with $H^{(2)}$,
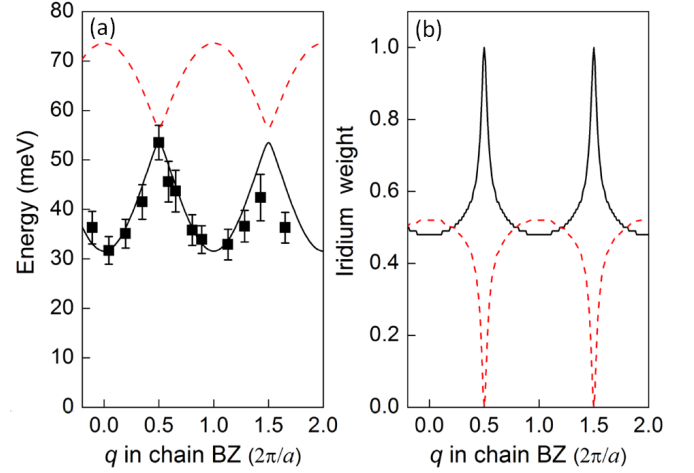

FIG. 4. (a) Calculated magnon dispersion (lines), compared with the experimental data (solid squares). (b) The Ir partial spectral weights for the lower (solid line) and upper (dashed line) branches in (a). $J_1 = 21$ meV, $\gamma_1 J_1 = 53.5$ meV, $J_2 = 2.4$ meV, $\gamma_2 J_2 = 0.6$ meV are used, which satisfy the theoretic constraints [22].

the latter method yields [22]:

$$\omega_{\mp}(q) = \frac{1}{2}[2\gamma_1 J_1 + \gamma_2 J_2 - J_2 \cos(qa)]$$
$$\mp \frac{1}{2}\sqrt{[\gamma_2 J_2 - J_2 \cos(qa)]^2 + 4J_1^2 \cos^2(qa/2)}.$$

The second-neighbor interaction opens another gap of size $(1+\gamma_2)J_2$ at $q = \pi/a$ in the middle of the band. The lower branch $\omega_-(q)$ can be fit in good agreement to the experimental data, as shown in Fig. 4(a).

The missing of the upper branch $\omega_+(q)$ spanning from 55 to 75 meV in our RIXS data has two implications. One, there exists a channel for the single-magnon excitation at $\omega_+(q)$ to decay into the two-magnon continuum, which starts at about 60 meV (twice the single-magnon spectral gap), or the multi-magnon bound states, which lie around 50 meV [22]. Due to strong SOC at Ir sites, lattice irregularities could act as an effective magnetic field applying on the isospins; such random magnetic field can lead to the decay. This scenario agrees with the previous observation of defect-induced spin-glass behavior in this material [27].

The other implication is called for the possible insufficiency of the decay near the zone boundary $q = \pi/a$, where $\omega_+(q)$ is very close to $\omega_-(q)$. It is likely that since the RIXS data were taken at the Ir L_3 edge, only the Ir weight is visible. The weights of Ir character [22] in the lower $(-)$ and upper $(+)$ branch of the spin-wave dispersion, $I_{\mp}(q)$, are shown in Fig. 4(b). Overall, $I_-(q)$ (solid line) is much larger than $I_+(q)$ (dashed line) and it follows the chain BZ, in agreement with the RIXS data. Note that it is the tiny J_2 that dramatically changes the weight distribution; otherwise $I_{\mp}(q) \equiv 1/2$ for $J_2 = 0$.

Although this argument alone is not adequate near the zone center, where both $I_\pm(q=0) \simeq 1/2$, the band top nature of $\omega_+(q=0)$ implies a strong decay there—both implications are at work to yield the invisibility of $\omega_+(q)$ in our experiment. For a direct experimental verification of the above arguments, we note that $\omega_+(q=\pi/a)$ has the full Cu weight (the Cu partial spectral weight is $1-I_\mp(q)$ by the sum rule). Hence, $\omega_+(q)$ should be detectable by the near zone boundary Cu L_3 edge RIXS [28] and this will be pursued in the feature [29].

In summary, we have presented a combined experimental and theoretical study of the unusual ferromagnetism in Sr_3CuIrO_6. We have consistently revealed a strongly anisotropic spin dynamics in this material, and found that an unusual exchange anisotropy generating mechanism, namely strong ferromagnetic anisotropy arising from antiferromagnetic superexchange, is generally present in the system with edge-sharing $Cu^{2+}O_4$ plaquettes and $Ir^{4+}O_6$ octahedra. Our results demonstrate that mixed $3d-5d$ compounds can generate distinct exchange pathways and thus novel magnetic behavior that are absent in pure $3d$ or $5d$ compounds.

_____

* wyin@bnl.gov

[1] E. Dagotto, Science, **309**, 257 (2005).
[2] B. J. Kim, H. Ohsumi, T. Komesu, S. Sakai, T. Morita, H. Takagi, and T. Arima, Science, **323**, 1329 (2009).
[3] B. J. Kim, H. Jin, S. J. Moon, J.-Y. Kim, B.-G. Park, C. S. Leem, J. Yu, T. Noh, C. Kim, S.-J. Oh, J.-H. Park, V. Durairaj, G. Cao, and E. Rotenberg, Phys. Rev. Lett., **101**, 076402 (2008).
[4] S. J. Moon, H. Jin, K. Kim, W. S. Choi, Y. S. Lee, J. Yu, G. Cao, A. Sumi, H. Funakubo, C. Bernhard, and T. Noh, Phys. Rev. Lett., **101**, 226402 (2008).
[5] J. Kim, D. Casa, M. H. Upton, T. Gog, Y.-J. Kim, J. F. Mitchell, M. van Veenendaal, M. Daghofer, J. van den Brink, G. Khaliullin, and B. J. Kim, Phys. Rev. Lett., **108**, 177003 (2012).
[6] D. Pesin and L. Balents, Nature Phys., **6**, 376 (2010).
[7] G. Jackeli and G. Khaliullin, Phys. Rev. Lett., **102**, 017205 (2009).
[8] Y. Singh, S. Manni, J. Reuther, T. Berlijn, R. Thomale, W. Ku, S. Trebst, and P. Gegenwart, Phys. Rev. Lett., **108**, 127203 (2012).
[9] X. Liu, T. Berlijn, W.-G. Yin, W. Ku, A. Tsvelik, Y.-J. Kim, H. Gretarsson, Y. Singh, P. Gegenwart, and J. P. Hill, Phys. Rev. B, **83**, 220403(R) (2011).
[10] S. K. Choi, R. Coldea, A. N. Kolmogorov, T. Lancaster, I. I. Mazin, S. J. Blundell, P. G. Radaelli, Y. Singh, P. Gegenwart, K. R. Choi, S.-W. Cheong, P. J. Baker, C. Stock, and J. Taylor, Phys. Rev. Lett., **108**, 127204 (2012).
[11] F. Ye, S. Chi, H. Cao, B. C. Chakoumakos, J. A. Fernandez-Baca, R. Custelcean, T. F. Qi, O. B. Korneta, and G. Cao, Phys. Rev. B, **85**, 180403(R) (2012).
[12] J. Kim, Y. Choi, J. Kim, J. F. Mitchell, G. Jackeli, M. Daghofer, J. van den Brink, G. Khaliullin, and B. J. Kim, Phys. Rev. Lett., **109**, 037204 (2012).
[13] R. Arita, J. Kuneš, A. Kozhevnikov, A. G. Eguiluz, and M. Imada, Phys. Rev. Lett., **108**, 086403 (2012).
[14] X. Liu, V. M. Katukuri, L. Hozoi, W.-G. Yin, M. P. M. Dean, M. H. Upton, J. Kim, D. Casa, A. Said, T. Gog, T. Qi, G. Cao, A. M. Tsvelik, J. van den Brink, and J. P. Hill, Phys. Rev. Lett., **109**, 157401 (2012).
[15] A. Kitaev, Ann. Phys. (N.Y.), **321**, 2 (2006).
[16] T. N. Nguyen, P. A. Lee, and H.-C. zur Loye, Science, **271**, 489 (1996).
[17] T. N. Nguyen and H.-C. zur Loye, J. Solid State Chem., **117**, 300 (1995).
[18] L. J. Ament, M. van Veenendaal, T. P. Devereaux, J. P. Hill, and J. van den Brink, Rev. Mod. Phys., **83**, 705 (2011).
[19] C. Lampe-Önnerud, M. Sigrist, and H.-C. zur Loye, J. Solid State Chem., **127**, 25 (1996).
[20] C. N. Yang and C. P. Yang, Phys. Rev., **151**, 258 (1966).
[21] J. D. Cloizer and M. Gaudin, J. Math. Phys., **7**, 1384 (1966).
[22] See Supplementary Material at [http://link.aps.org/supplemental/xxxxxxxxx] for technical details.
[23] J. Kanamori, J. Phys. Chem. Solids, **10**, 87 (1959).
[24] P. W. Anderson, Phys. Rev., **79**, 350 (1950).
[25] O. Kahn, J. Galy, Y. Journaux, J. Jaud, and I. Morgenstern-Badarau, J. Am. Chem. Soc., **104**, 2165 (1982).
[26] J. Kanamori, Prog. Theor. Phys. **17**, 177 (1957).
[27] A. Niazi, E. V. Sampathkumaran, P. L. Paulose, D. Eckert, A. Handstein, and K.-H. Müller, Phys. Rev. B, **65**, 064418 (2002).
[28] M. P. M. Dean, R. S. Springell, C. Monney, K. J. Zhou, J. Pereiro, I. Božović, B. D. Piazza, H. M. Rnnow, E. Morenzoni, J. van den Brink, T. Schmitt, and J. P. Hill, Nature Mater., **11**, 850 (2012).
[29] To date, the energy resolution of Cu L_3 edge RIXS is about 130 meV for practical use, which is not good enough to discern the magnetic excitations $\sim$ 60 meV in this material. Facilities expected to operate with 10 meV resolution are under construction, for example, at Brookhaven National Laboratory as part of NSLS II.